OBSERVATION OF *d-d* FUSION NEUTRONS DURING DEGASSING OF DEUTERIUM-LOADED PALLADIUM

COLD FUSION

TECHNICAL NOTE

KEYWORDS: *d-d fusion neutrons, palladium, deuterium expulsion*

MICHAEL BITTNER, ANDREAS MEISTER, DIETER SEELIGER, RAINER SCHWIERZ, and PETER WÜSTNER

Dresden University of Technology, Institute for Nuclear and Atomic Physics
Mommsenstrasse 13, O-8027 Dresden, Germany

Received July 31, 1991
Accepted for Publication August 3, 1992

Experiments with two massive deuterium-loaded palladium samples designed to search for deuteron-deuteron (d-d) fusion during thermal degassing are described. In the heavier of the two samples, which has a total mass of ~0.5 kg, during deuterium expulsion from the metal, a significant neutron excess count rate was detected by two independent NE-213 scintillation neutron detectors. The maximum time-dependent excess count rate corresponds to a d-d reaction rate of $(3 \pm 1) \times 10^{-25}$ *per deuteron pair per second. From detector pulse high spectra, the energy of the neutrons is determined to be ~2.5 MeV, as expected for d-d fusion neutrons.*

INTRODUCTION

Many experiments in which palladium is charged with deuterium, either electrolytically or by gas absorption, indicate production of fast neutrons or other products of deuteron-deuteron (*d-d*) fusion reactions accompanying the charging process under special, hitherto not fully understood conditions. Some experiments indicate very weak, rather continuous neutron production, whereas in other experiments, short intense neutron bursts are indicated, for example, Ref. 1. These results need further work toward experimental confirmation and understanding of the underlying physical processes.

At the Dresden University of Technology, after a first experiment confirming very weak neutron production during electrolytic charging of palladium cathodes with deuterium,[2] some further studies on the phenomenon of nuclear fusion in condensed matter were carried out that systematically hint at weak neutron production as a typical function of the period of charging.[3-5] For massive probes, these measurements are very time-consuming.

The experiments described in this technical note are designed to search for neutron events during the degassing of palladium samples charged with deuterium. Of special interest is the search for neutrons with an energy of 2.45 MeV, originating from the following fusion reaction:

$$d + d \rightarrow n + {}^3\mathrm{He} + 3.27\ \mathrm{MeV}\ .$$

In this case, the physical processes of *d-d* fusion in the palladium lattice should be similar to those during electrochemical charging. But, degassing carried out at higher temperature leads to a much higher mobility of the deuterons in the lattice, to more deuterons located in the interstitial plasma, and to somewhat higher deuteron kinetic energies. All these effects are expected to increase low-energy deuterium fusion. Furthermore, thermal degassing is many times faster than electrochemical charging of massive palladium samples. This favors a degassing measurement from the experimental point of view because the duration of the experiment is shorter, and the constancy of both background and detector stability are not as problematic as in long-term experiments.

EXPERIMENT

In these experiments, two massive palladium samples are used, in which deuterium was stored. These deuterium-loaded palladium samples are heated on an electrical heating device in front of a neutron detector. Figure 1 presents the experimental arrangement. The principal geometry with two independent detectors for two sample positions is shown in Fig. 1a, and the more detailed design of the near detector assembly with heating device is given in Fig. 1b.

The measurements are carried out in short time runs of 10 min each with the sample placed alternately in position 1 or 2. While the sample is observed with one detector, the other detector registers the background count rate for the empty position. The effective count rate is small enough, as is seen later, to avoid any remarkable influence of the sample on the count rate of the detector at the empty position. In this manner, alternatively with two detectors, the effect and the background count rate are measured quasi-simultaneously for the entire period of the experiments. This is an essential feature of these experiments because this procedure provides a good check of the reproducibility of the measured data and shows the reliability of the results of these low-level counting measurements.

For neutron detection and spectrometry, two recoil-proton detectors with 5-in.-diam × 1.5-in.-high NE-213 liquid scintillators coupled to XP-2040 photomultipliers are used. The pulse high spectra of these detectors are recorded by multichannel analyzers with 512 channels. The electronic circuit includes pulse-shape discrimination for separation of gamma

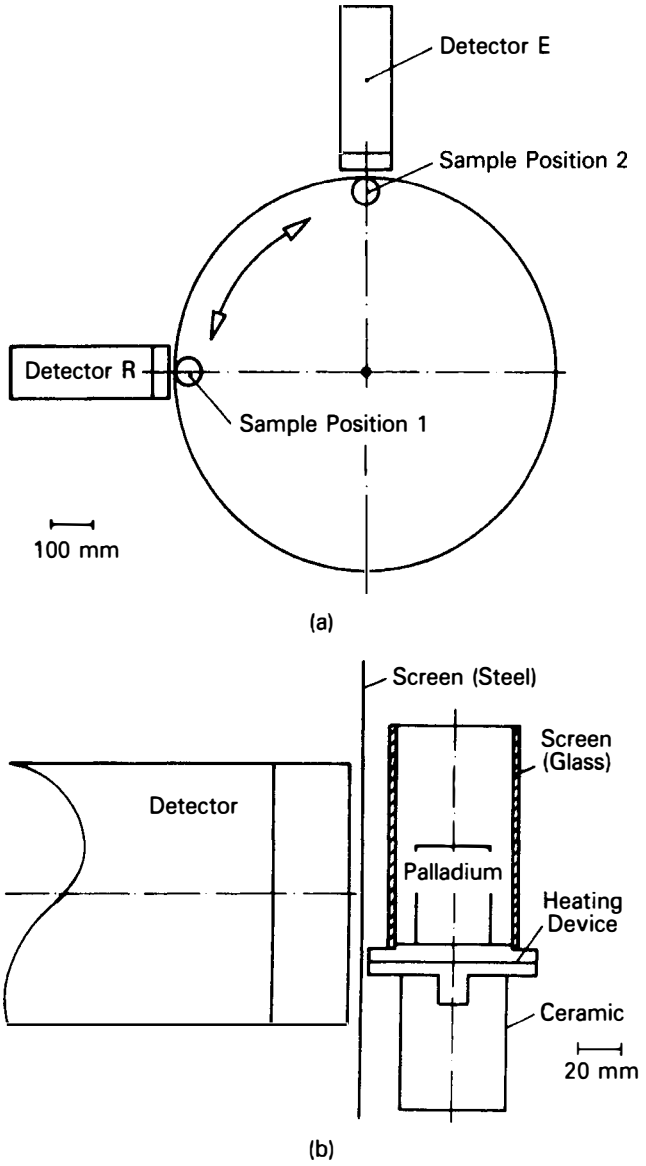

Fig. 1. Schematic of (a) the experimental arrangement and (b) the degassing device.

events. This guarantees suppression of the gamma events by a factor of 2×10^{-4} (detector R) and 5×10^{-4} (detector E) for pulse highs corresponding to 2- to 5-MeV neutron energy. The spectrometer is explained in more detail in Ref. 3.

To further reduce the background, the experimental setup is surrounded by shielding consisting of ~50 cm of polyethylene and water. This shielding reduces the background in the energy interval of interest to about one-fourth, as compared with measurements carried out with the same equipment but without shielding.

Before the degassing experiments, the two cylindrical palladium samples (Z6 and Z8) were loaded cathodically with deuterium by electrolysis of heavy water for 1154 h with a current of 4 A (Z6) and for 1254 h with 8 A (Z8). The electrolyte was a solution of 1 *M* LiOD in heavy water enriched to 90% in D_2O.

Table I shows the sample masses before charging, after electrochemical charging with deuterium, after the thermal degassing, and 1 month later. The deuterium inventory in the samples can be determined from the mass differences. From this follow average hydrogen-to-palladium atom ratios of 0.74 ± 0.05 (Z6) and 0.80 ± 0.01 (Z8) after the electrochemical charging. These values are determined assuming that the deuterium content of the absorbed hydrogen is 90% as it is in the electrolyte. The masses given in Table I also include the mass of a wire for conducting the electric current, which is fixed to each of the samples. A comparison of the masses in Table I shows that practically all the deuterium leaves the samples during the degassing experiments.

For degassing, the samples are situated on an electric heater with 450 W of heating power. During this procedure, the samples are in normal contact with air. The heating position is surrounded by a heat shield made of quartz glass. A 1-mm-thick steel plate is used between the heating device and detector as an additional heat shield to prevent the detectors from warming up.

We degassed Sample Z8 by placing it on the already heated plate. The sample was then observed for a total of 205 min in 18 short measuring runs. The overall duration of the experiment including all short time measurements was 264 min. The temperature was measured by a thermometer after heating for an asymptotic long time after degassing. The temperatures on the surface of the heating plate and on the top of sample Z8 were 375 and 205°C, respectively.

In the second experiment, sample Z6 was degassed, but this time starting at room temperature, then switching on the heating device. The sample was observed for a total of 124 min in 11 short measuring runs.

EXPERIMENTAL RESULTS

Figure 2 shows the pulse high spectrum accumulated with one of the detectors. This spectrum is the sum for all 22 short time runs with and without a sample, taken with detector E

TABLE I

Sample Shapes and Masses

	Sample Z6	Sample Z8
Shape	22-m-diam × 18-mm-high cylinder	34.7-mm-diam × 45.4-mm-high cylinder
Mass unloaded (g)	86.327	518.207
Mass after charging (g)	87.445	525.594
Mass after degassing (g)	86.405	518.303
Mass 1 month after degassing (g)	86.381	518.155

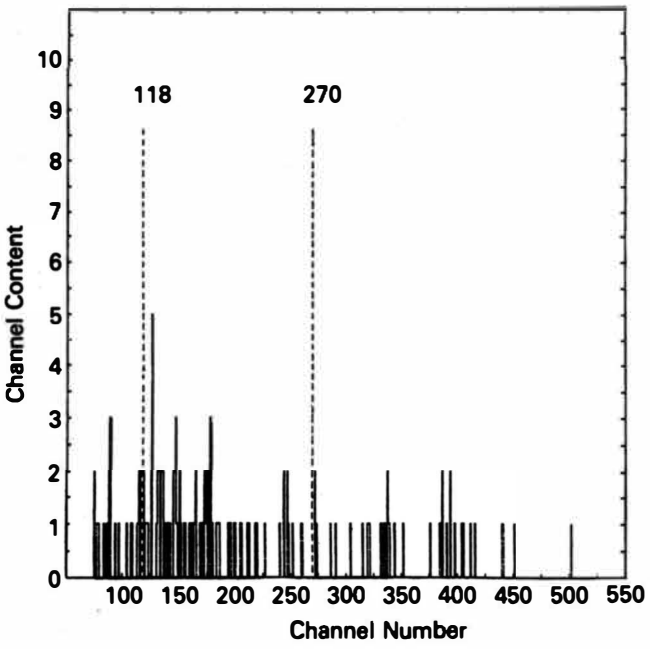

Fig. 2. Pulse high spectrum accumulated for all measurements with and without sample Z8 using detector E.

in the experiment with sample Z8. There is an electronic cutoff at channel 80. This is due to the energy threshold for the neutron/gamma discrimination circuit. The spectrum is therefore analyzed only for channels where the influence of this threshold becomes negligible. Because of counting statistics, two broad channel intervals are used to obtain satisfactory statistics: from 118 to 270, as shown in Fig. 2, and 271 to 511, corresponding to recoil-proton energy intervals of 1.9 to 3.3 MeV and 3.3 to 5.2 MeV, respectively.

Consequently, neutrons with energies below 3.3 MeV can be detected only in the first energy interval, whereas neutrons with energies above 3.3 MeV are detected in both intervals. The energy calibration is carried out with neutrons near 2.5 and 14 MeV at a neutron generator utilizing the *d-d* and *d-t* reactions, respectively. Between these two energies and below 2.5 MeV, the light output is interpolated by the light output function for an NE-213 scintillator given in Ref. 6.

The measured count rates are displayed in Fig. 3 for both detectors and both energy intervals. The hatched sections of the histograms indicate measurements with sample Z8 in front of the detector, whereas the clear sections are count rates for measurements with an empty position in front of the detector. Four of these "empty" measurements, two before and two after the degassing measurements, are carried out with the heating device in front of the detectors to be sure that it does not influence the detectors. Ten minutes after

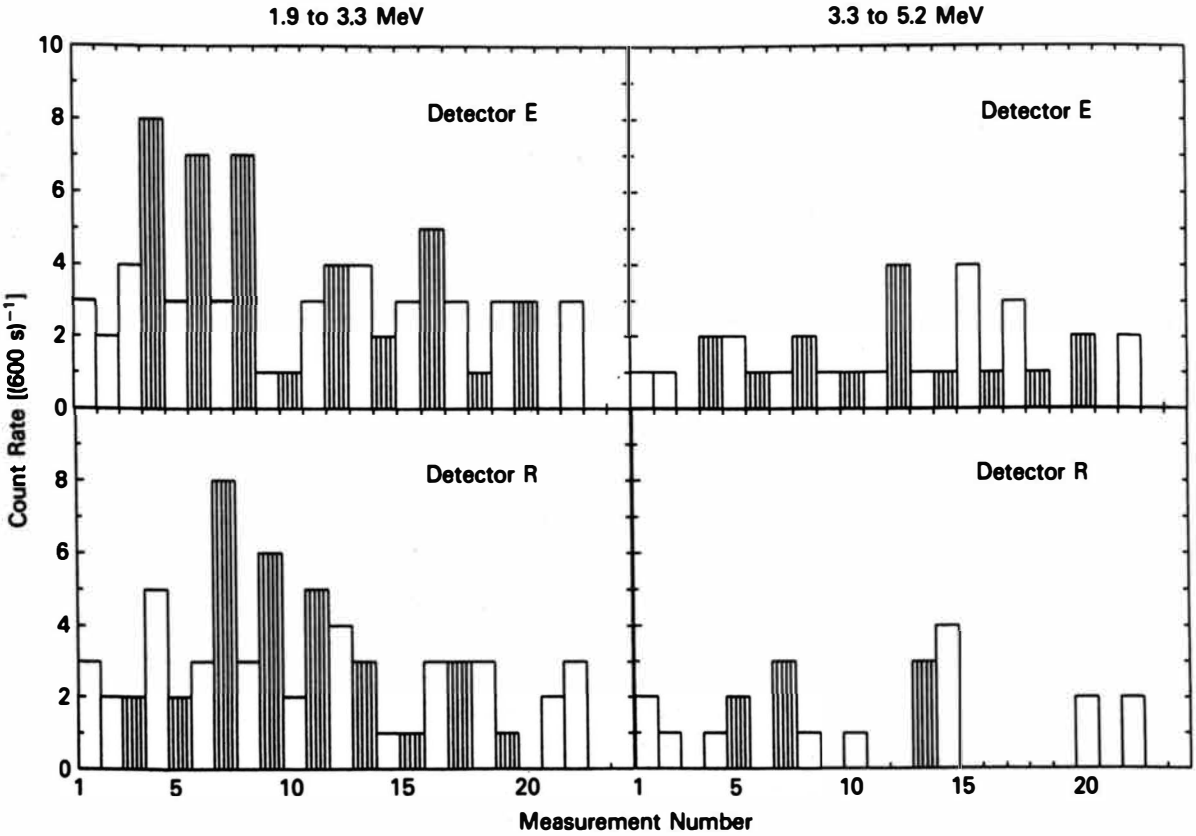

Fig. 3. Count rates for the experiments with sample Z8 within the recoil-proton energy intervals of 1.9 to 3.3 MeV and 3.3 to 5.2 MeV from both detectors. The hatched sections of the histograms are measurements with the sample; the clear sections are without the sample.

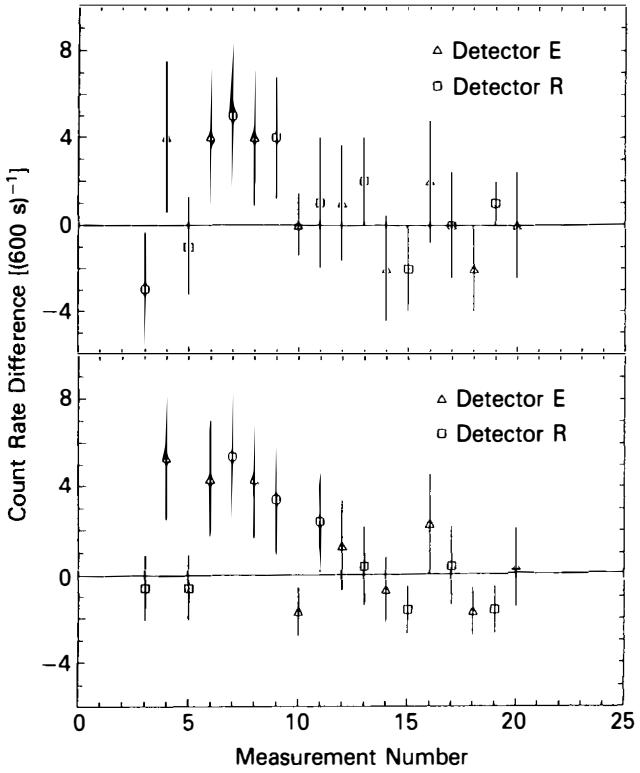

Fig. 4. Difference in count rates between measurements with sample Z8 and the temporal neighboring measurement without sample (upper part) as well as for an averaged background count rate (lower part).

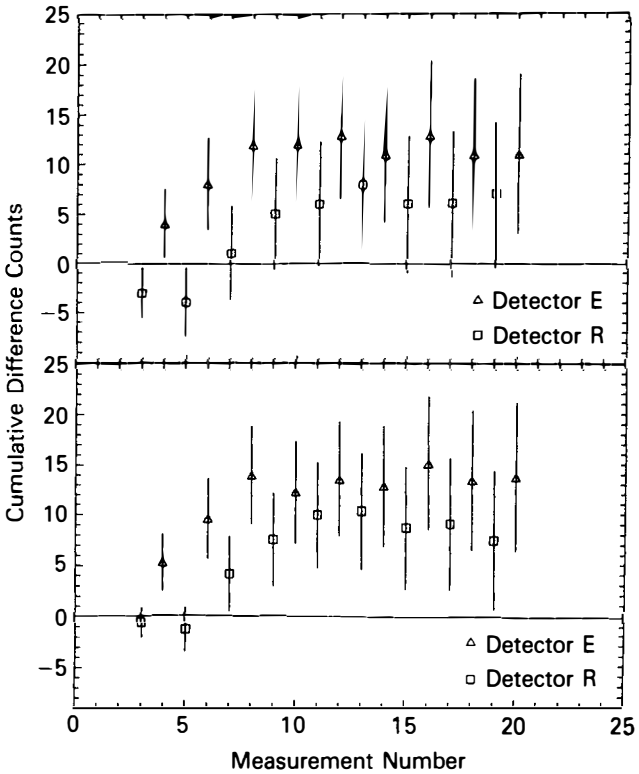

Fig. 5. Cumulative difference counts for sample Z8 minus background: individual background (upper part) and averaged background line (lower part), accumulated up to the actual measurement.

sample Z8 was placed on the heating device, a short oxyhydrogen gas reaction *t* took place that did not interrupt the measurements, however.

In the 1.9- to 3.3-MeV energy range, both detectors indicate count rates within some of the measuring runs after the start of degassing that are significantly above the background. Later, after the 13th run, no difference between measurements with and without a sample would be found. In the 3.3- to 5.2-MeV energy range, no measurements indicate any difference between effect and background outside the statistical uncertainties.

The count rate differences for measurements with and without a sample are shown in Fig. 4. The background is determined in two different ways. First, every run with a sample was compared with the neighboring run without a sample (upper part of Fig. 4). Second, an average background count rate is used, which is the average over all runs without a sample (lower part of Fig. 4). Independently of these two methods of background determination, a maximum excess count rate of ~4 count/10 min above the background is indicated by both detectors within the same time interval. An accumulation of these difference count rates from the degassing up to the actual run is given in Fig. 5. They are determined with individual background measurements as well as an averaged background line. These cumulative difference counts rise until the ninth measurement and then fluctuate around a constant value with a growing magnitude of fluctuation, indicating that effects are observed only within the first half of the experimental period.

The results for sample Z8 give rise to the assumption that neutrons occur within the sample for ~100 min after the beginning of the degassing. The results for the smaller sample Z6, however, are different from those of sample Z8. Figure 6 gives the count rates for Z6 in the same manner as was done for Z8 in Fig. 3. Evidently, there are no deviations from the background measurements. Figure 7 also gives the count rate differences for the measurements with and without a sample for both detectors. Also in this representation, only the counting statistics around zero are seen.

DISCUSSION

First, we discuss an attempt to determine the recoil-proton spectrum within the time interval between the fourth and the ninth measurements, when the count rate difference for sample Z8 is at a maximum. To determine the background, all the other 38 measurements are used to obtain the best counting statistics possible. The background therefore includes all measurements without a sample plus the measurements 10 through 20 with a sample, when the excess count rate becomes negligible.

Figure 8 shows the recoil-proton spectrum within 0.5-MeV energy bins. The nonlinear proton light output is accounted for as mentioned earlier. For comparison, Fig. 8 also includes a recoil-proton spectrum measured with good statistics for 2.48-MeV neutrons from the *d-d* reaction at a neutron generator (perpendicular to the beam axis). The absolute high of this spectrum is chosen to fit the spectrum belonging to Z8. The agreement between both spectra is very good. From this it can be concluded that the energy of the neutrons detected

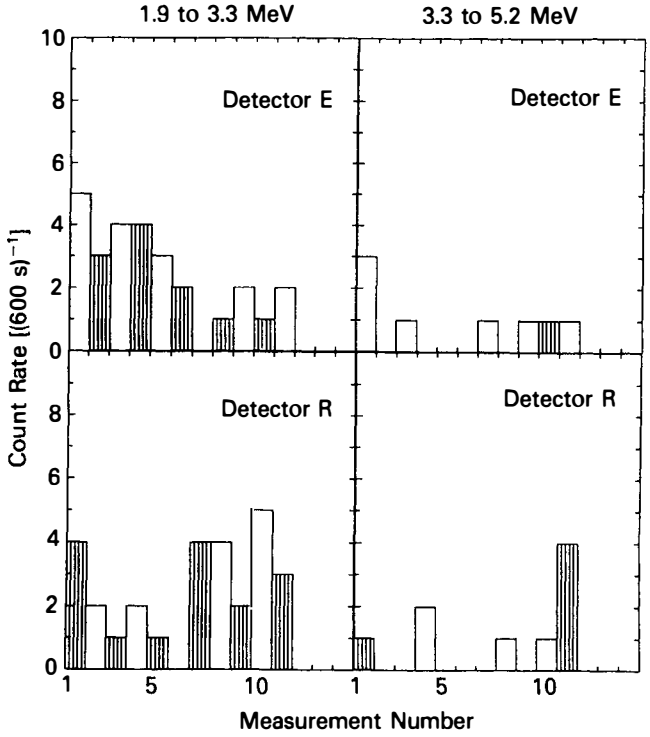

Fig. 6. Count rates for the experiments with sample Z6 within the recoil-proton energy intervals of 1.9 to 3.3 MeV and 3.3 to 5.2 MeV from both detectors. The hatched sections are measurements with sample; the clear sections are without the sample.

during the degassing of sample Z8 is ~2.5 MeV. This confirms the assumption that these neutrons originate from *d-d* fusion.

A surprising experimental result is the difference in behavior of samples Z8 and Z6: Whereas neutron events near 2.5 MeV are indicated from sample Z8, this is not so for Z6. But, the samples are distinguished mainly by their different masses, which is assumed to be the reason for the differences in behavior.

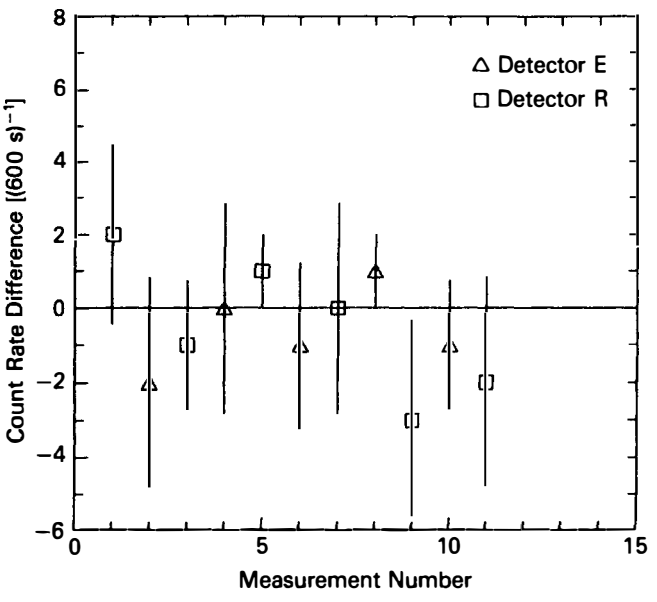

Fig. 7. Count rate differences for measurements with and without sample Z6.

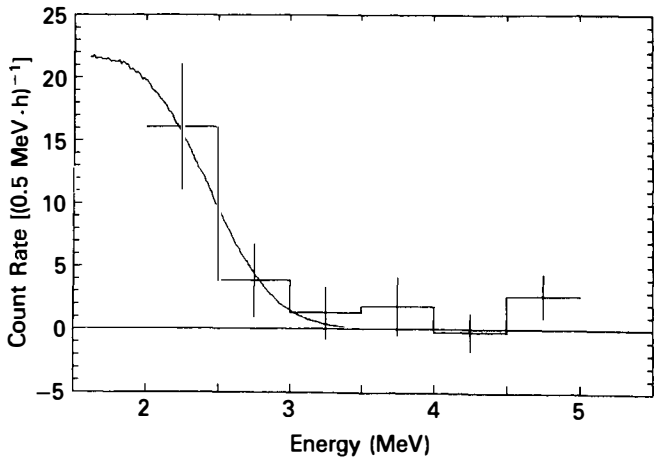

Fig. 8. Proton-recoil spectrum during degassing of sample Z8 (measurements 4 through 9) with 0.5-MeV energy bins and spectrum for 2.48-MeV neutrons from *d-d* reaction at a neutron generator (curve).

For comparison, the experimental data should be expressed in terms of nuclear reaction events per deuteron pair per second by

$$\lambda_{d\text{-}d} = \frac{\dot{N}_s - \dot{N}_b}{\epsilon} \cdot \frac{2 \cdot M_D}{m_D \cdot L} ,$$

as done in many papers, following the deuteron pair fusion model from Ref. 7, where

m_D = absorbed deuterium mass; for simplicity, m_D is taken to be the maximum value before degassing

M_D = mass of 1 mol of deuterium (2.014 g)

L = Avogadro's number (6.02×10^{23} atoms)

ϵ = detection efficiency for neutrons originating in the sample. (The detection efficiency was calculated by a Monte Carlo code. Including the actual sample-detector geometry, it amounts to 0.023 for 2.45-MeV neutrons.)

From measurements 4 through 9 with sample Z8, when the effect is near its maximum, $\lambda_{d\text{-}d} = (3 \pm 1) \times 10^{-25}$ per deuteron pair per second. This value is of the same order as our results from previous experiments on neutron production during electrochemical loading of palladium samples with deuterium.[2-5] As in our previous analysis using a simple plasma model,[8] *d-d* neutron production becomes observable only during nonequilibrium conditions.

From measurements with sample Z6, an upper limit for $\lambda_{d\text{-}d}$ can be estimated. Starting from the 1σ statistical error of a single short time run (±1.6 count/10 min) as a minimal observable effect, this yields $\lambda_{d\text{-}d} < 10^{-24}$ per deuteron pair per second. This means that the registration limit for deuterium nuclear reactions in the experiment with the smaller sample Z6 is not sufficient for its detection at the given background rate. From this point of view, the results from samples Z8 and Z6 are not incompatible if the reaction rate is

proportional to the number n of deuterons in the palladium sample (or to any function n^κ where $\kappa > 1$). The latter is suitable, e.g., for fusion in a plasma, when the reaction rate is proportional to n^2 (see Ref. 8).

Furthermore, it is interesting to compare the time dependence of the observed reaction rate for Z8 with the actual deuterium content of the sample. To this end, calculations are carried out using a model for deuterium liberation based on the gas diffusion in palladium. This model is explained in more detail in the Appendix. Because of some simplifying assumptions in the model and a lack of precise input data, the calculations are carried out with variations in the parameters determining the time behavior of the degassing process. Table II gives three parameter sets, for which the results of calculations are shown in Fig. 9 in comparison with experimental reaction rates $\dot{N}^{d\text{-}d}$ determined as

$$\dot{N}^{d\text{-}d} = \frac{\dot{N}_s - \dot{N}_b}{\epsilon} .$$

All the represented calculations reproduce very well the experimental fact that after 200 min, only a very small amount of deuterium remains in the sample. If the chemical reaction energy from catalytic oxidation of escaping deuterium were not accounted for, that is, $\alpha_{ch} = 0$, then the deuterium content in the sample after 200 min would be ~50% of the initial content m_0, which is in serious contradiction with the weighed masses. Certainly, the calculations include only continuous degassing, and not sporadic material cracks, gas eruptions, changes in the catalytic activity of sample surface, etc. Therefore, they can only reproduce the mean behavior in a general way. Figure 9 also shows the calculated temperature curves belonging to the degassing curves. Sample Z8, except the wire affixed to it, did not show temperature color during the course of degassing, so that the temperature could not be much higher than 600°C. Hence, the three temperature plots reproduce to some extent an appropriate temperature course.

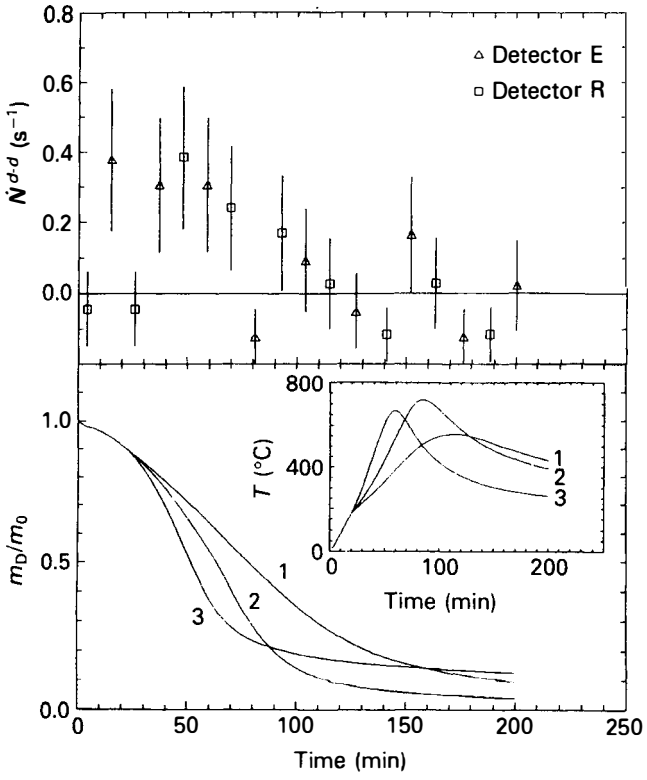

Fig. 9. Time dependence of experimental reaction rate $\dot{N}^{d\text{-}d}$ (upper part) in comparison with the deuterium content in sample Z8 (lower part). The deuterium content m_D/m_0 is calculated with the parameters given in Table II. A plot of calculated sample temperature T is inserted.

TABLE II

Parameter Sets for Calculation of Thermal Deuteron Liberation from Sample Z8

Set	T_0 (°C)	α_{ch}	β
1	205	0.3	0.05
2	205	0.4	0.05
3	205	0.6	0.3

A comparison of the time characteristics of deuterium content with the measured reaction rates shows that the deuterium content decreases to small values after 50 to 100 min; in parallel with this, the reaction rate also vanishes. This indicates a correlation between the quantities and implies that the registered events are caused by deuterium nuclear reactions. A further conclusion can be drawn concerning the background determination, which is done by measuring for an empty position instead of an undeuterated control sample. About half the measurements with sample Z8 (after measurement 12) were done with only a small deuterium content. These measurements show that there is no influence of the undeuterated large palladium sample on the detector count rate by other factors, e.g., by cosmic-ray spallation reactions in the sample, which would cause the observed excess neutron count rate.

Calculations for the lighter sample Z6 with the parameter sets given in Table II yield a time behavior of deuterium liberation similar to that for Z8. Therefore, the reaction events in Z6 are also expected to be shared within a period of ~1 h, not concentrated within a short period of only some minutes.

CONCLUSION

Experiments with a 0.5-kg palladium sample show a definite excess neutron count rate for a period of ~1 h. This is just the time interval during which the deuterium is expelled from the massive palladium sample. The energy of the detected neutrons is near 2.5 MeV, as expected for *d-d* fusion neutrons. Therefore, the conclusion is obvious: These neutrons are caused by the *d-d* fusion reaction. The excess neutron count rate, which is time dependent, corresponds at its maximum to a *d-d* reaction rate of $(3 \pm 1) \times 10^{-25}$ per second per deuteron pair.

APPENDIX

CALCULATION OF THERMAL DEUTERIUM LIBERATION FROM A MASSIVE PALLADIUM SAMPLE

The thermal expulsion of deuterium from a massive deuterium-loaded palladium sample is determined essentially by

diffusion of deuterium in the palladium lattice, and diffusion depends very strongly on temperature. The deuterium released from the palladium sample can be catalytically oxidized at the palladium surface because of the presence of oxygen under the open air condition as in the experiments discussed here. The chemical reaction

$$2 \cdot D_2 + O_2 \rightarrow 2 \cdot D_2O$$

proceeds with an excess enthalpy of 147.3 kJ/mol deuterium.[9] This combustion energy causes an increase in the sample temperature, which additionally increases the diffusion velocity.

To model the thermal liberation of deuterium from a deuterium-loaded sample, we use a model where the sample is situated within the surroundings of a given constant temperature T_0. The shape of the sample is approximated by a sphere of equal volume. Figure A.1 illustrates the features of this model, which is explained in the following.

The diffusion equation for the deuterium concentration n_D in the palladium lattice,

$$\frac{dn_D(t,r)}{dt} = D(T)\nabla^2 n_D(t,r) \ ,$$

is solved initially for an even concentration profile n_0 within the whole sphere,

$$n_D(t=0,r) = n_0 \ ,$$

and a permanently zero concentration outside the sphere with radius R,

$$n_D(t,r>R) = 0 \ .$$

The deuterium mass m_D in the sample at time t is then obtained by integration of $n_D(r,t)$ over the sphere volume:

$$m_D(t) = \int_V dV \, n_D(r,t) \ .$$

The escaping deuterium gas can be catalytically oxidized at the palladium surface, at least partially, and the combustion heat warms the sample. The portion α_{ch} of chemical energy utilized for heating is, for simplicity, assumed to be constant during the entire degassing period. Moreover, the resulting increase in the sample temperature is determined by the heat transfer to the surroundings and the heat capacity C of the sample. The heat transfer is assumed to be black body radiation as described by the Stefan-Boltzmann law with the surroundings as the black body of temperature T_0 and the sample as the gray body of temperature T and emissivity β of its surface. With these assumptions, the heat balance can be written in terms of the sample temperature T as follows:

$$\frac{dT}{dt} = \frac{\alpha_{ch} W_{ch}}{M_D C} \frac{dm_D}{dt} - \frac{4\pi R^2 \gamma \beta (T^4 - T_0^4)}{C} \ ,$$

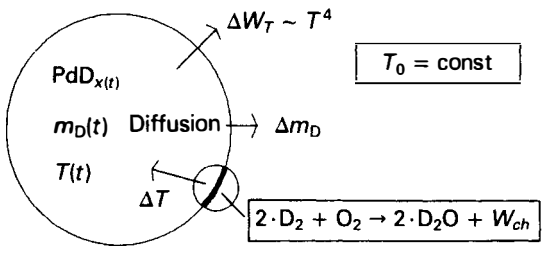

Fig. A.1. Model for thermal deuterium liberation from a massive palladium sample.

where γ is the Stefan-Boltzmann constant (5.7×10^{-8} W/$m^2 \cdot K^4$).

Data are needed for the parameters $D(T)$, α_{ch}, β, and C. The diffusion constant $D(T)$ is taken from experimental values collected in Ref. 10 and interpolated for the actual temperature. For simplicity, the concentration dependence of the diffusion constant D is neglected.

The parameter α_{ch} considers catalytic recombination of the deuterium. It is varied to describe the weighed deuterium content remaining in the sample after degassing and the maximum sample temperature. The value α_{ch} is expected to depend on the catalytic activity of the sample surface.[9] It can be expected to be neither constant nor reproducible during the degassing process.

The thermal emissivity β is ~0.02 to 0.05 for polished metals, and ~0.6 for oxidized metals, and it depends on temperature. The surface of sample Z8 could not be classified unambiguously as metallic or oxidized. It was partially metallic and partially coated with a surface layer. Therefore, this value is also varied to determine its influence on the results.

The heat capacity C of the samples was estimated as 25 J/K per mole of palladium or deuterium and superposed for both components.

ACKNOWLEDGMENTS

The authors appreciate the help and assistance of B. Altmann and E. Paffrath.

REFERENCES

1. J. O'M. BOCKRIS, G. H. LIN, and N. J. C. PACKHAM, "A Review of the Investigations of the Fleischmann-Pons Phenomena," *Fusion Technol.*, **18**, 11 (1990).

2. D. SEELIGER et al., "Search for DD-Fusion Neutrons During Heavy Water Electrolysis," *Electrochim. Acta*, **34**, 991 (1989).

3. M. BITTNER et al., "Method for Investigation of Fusion Reactions in Condensed Matter," *Fusion Technol.*, **18**, 120 (1990).

4. M. BITTNER et al., "Evidence for the Production of *d-d* Fusion Neutrons During Electrolytic Infusion of Deuterons into a Palladium Cylinder," *Fusion Technol.*, **19**, 2119 (1991).

5. M. BITTNER et al., "Indication for the Temporary Production of *d-d* Fusion Neutrons During Electrolytic Infusion of Deuterons into a Massive Palladium Slab," *Fusion Technol.*, **20**, 334 (1991).

6. R. A. CECIL, B. D. ANDERSON, and R. MADEY, "Improved Predictions of Neutron Detection Efficiency for Hydrocarbon Scintillators from 1 MeV to About 300 MeV," *Nucl. Instrum. Methods*, **161**, 439 (1979).

7. S. E. JONES et al., "Observation of Cold Nuclear Fusion in Condensed Matter," *Nature*, **338**, 737 (1989).

8. D. SEELIGER and A. MEISTER, "A Simple Plasma Model for the Description of *d-d* Fusion in Condensed Matter," *Fusion Technol.*, **19**, 2114 (1991).

9. G. KREYSA, G. MARX, and W. PLIETH, "A Critical Analysis of Electrochemical Nuclear Fusion Experiments," *J. Electroanal. Chem.*, **266**, 437 (1989).

10. J. VÖLKL and G. ALEFELD, "Diffusion of Hydrogen in Metals," *Topics in Applied Physics, Hydrogen in Metals*, Vol. 28, G. ALEFELD and J. VÖLKL, Eds., Springer, Berlin (1978).